Studying Friction and Shear Fracture in Thin Confined Films Using a Rotational Shear Apparatus

Manoj K. Chaudhury* and Jun Young Chung†

Department of Chemical Engineering, Lehigh University, Bethlehem, Pennsylvania 18015

Received February 20, 2007. In Final Form: May 4, 2007

This paper describes the effects of the elastic modulus and sliding velocity on the friction and shear fracture of smooth silanized rigid disks rotating against thin confined films of poly(dimethylsiloxane) (PDMS) elastomers. A rigid glass disk is rotated against thin PDMS films of different thicknesses and moduli bonded to a glass plate at various speeds. While the disk rotates on the PDMS coated glass plate, a load cell measures the resulting force with a cantilever beam. One end of the cantilever beam is glued to the glass plate, while its other end presses against a load cell. From the balance of forces and torques, the friction force at a given slip velocity is determined. The friction force increases with the slip velocity sublinearly, which is consistent with the results reported previously by Vorvolakos and Chaudhury (*Langmuir* **2003**, *19*, 6778). During rotation, however, the glass disk comes off the PDMS film when the shear stress reaches a critical value. This critical shear stress increases with the modulus of the film, but it decreases with its thickness, following a square root relationship, which is similar to the adhesive fracture behavior in thin films under pull-off conditions. A simple model is presented that captures the essential physics of the fracture behavior under shear mode.

Introduction

Friction of polymeric materials is commonly measured by sliding a polymeric hemisphere against another substrate. Several investigators have used this method to study the kinetic friction of polymers against low-energy surfaces.[1−10] In these experiments, the width of the contact is much smaller than the size of the hemisphere; hence, the system is mechanically unconfined as opposed to the cases, such as thin films in contact with a flat surface, where the contact area is much larger than the thickness of the film. In our recent studies[4,7] with poly(dimethylsiloxane) (PDMS) hemispheres sliding against a smooth silanized silicon wafer, we observed that the friction force increases sublinearly with sliding velocity up to a critical value, beyond which the friction decreases, exhibiting a stick−slip motion as was observed earlier by Grosch[11] in a different system. It was suggested that the sublinear increase of friction is related to the stretching and relaxation of polymer chains, whereas the decrease of the friction beyond a critical velocity is due to the decrease of the numbers of polymer chains in the attached state.[12,13] More recently, Persson and Volokitin[14] applied a model of thermal fluctuation to the depinning of small contact patches at the rubber/substrate and theoretically reproduced many of the features of rubber friction as reported in refs 4 and 7. These models of friction involving either the fluctuation of polymeric molecules or that of the stress domain are restricted to a length scale no larger than a few nanometers. Hence, in thin films of micrometer level thickness but with large contact areas (i.e., so-called confined films), friction force should be independent of thickness with its value not being any different from those found in unconfined systems. However, a confined elastomeric film is prone to various types of interfacial instability.[15−19] A natural question, in this case, is whether these instabilities contribute to friction in any significant way. With these questions in mind, we devised a rotational shear method to study friction with thin confined films. A preliminary version of this experiment was reported previously by Ghatak and Chaudhury.[17] A rotational shear experiment was also used earlier by Gong et al.[20] in a different setting to study friction in thick gel films. The studies to be reported here have another objective, which is to shed some light on the removal of objects from surfaces in a twisting mode. As a result of the current experimental design, the rotating disk comes off the thin film at a critical shear stress. We try to understand how this critical shear stress depends on the modulus and the thickness of the polymer films.

Model System

The basic apparatus is shown schematically in Figure 1. Thin PDMS films of various shear moduli ($\mu = 0.26-3.1$ MPa) and thicknesses ($h = 38-406\ \mu$m) were prepared on rigid glass plates according to a method described previously.[17,21] These films were brought into contact with a silanized rigid borosilicate glass disk (3.8 mm radius and 1 mm thickness, Swift Glass Inc., Elmira,

* To whom correspondence should be addressed. E-mail: mkc4@lehigh.edu.

† Present address: Polymers Division, National Institute of Standards and Technology, Gaithersburg, Maryland 20899.

(1) Savkoor, A. R. *Wear* **1965**, *8*, 222.
(2) Bowden, F. P.; Tabor, D. *The Friction and Lubrication of Solids*; Clarendon Press: Oxford, 1950.
(3) Roberts, A. D.; Jackson, S. A. *Nature* **1975**, *257*, 118.
(4) Vorvolakos, K.; Chaudhury, M. K. *Langmuir* **2003**, *19*, 6778. The introduction of this paper describes the long history of the measurement of friction in polymers.
(5) Chaudhury, M. K.; Owen, M. J. *Langmuir* **1993**, *9*, 29.
(6) Brown, H. R. *Science* **1994**, *263*, 1411.
(7) Ghatak, A.; Vorvolakos, K.; She, H.; Malotky, D.; Chaudhury, M. K. *J. Phys. Chem. B* **2000**, *104*, 4018.
(8) Casoli, A.; Brendle, M.; Schultz, J.; Auroy, P.; Reiter, G. *Langmuir* **2001**, *17*, 388.
(9) Bureau, L.; Caroli, C.; Baumberger, T. *Phys. Rev. Lett.* **2006**, *97*, 225501.
(10) Yurdumakan, B.; Nanjundiah, K.; Dhinojwala, A. *J. Phys. Chem. C* **2007**, *111*, 960.
(11) Grosch, K. A. *Proc. R. Soc. London, Ser. A* **1963**, *274*, 21.
(12) Schallamach, A. *Wear* **1963**, *6*, 375.
(13) Chernyak, Y. B.; Leonov, A. I. *Wear* **1986**, *108*, 105.
(14) Persson, B. N. J.; Volokitin, A. I. *Eur. Phys. J. E* **2006**, *21*, 69.
(15) Ghatak, A.; Chaudhury, M. K.; Shenoy, V.; Sharma, A. *Phys. Rev. Lett.* **2000**, *85*, 4329.
(16) Mönch, W.; Herminghaus, S. *Europhys. Lett.* **2001**, *53*, 525.
(17) Ghatak, A.; Chaudhury, M. K. *Langmuir* **2003**, *19*, 2621.
(18) Ghatak, A.; Mahadevan, L.; Chung, J. Y.; Chaudhury, M. K.; Shenoy, V. *Proc. R. Soc. London, Ser. A* **2004**, *460*, 2725.
(19) Chung, J. Y.; Chaudhury, M. K. *J. R. Soc. Interface* **2005**, *2*, 55.
(20) Gong, J. P.; Kagata, G.; Osada, Y. *J. Phys. Chem. B* **1999**, *103*, 6007.
(21) Chung, J. Y.; Chaudhury, M. K. *J. Adhes.* **2005**, *81*, 1119.

10.1021/la700501m CCC: $37.00
Published on Web 06/16/2007

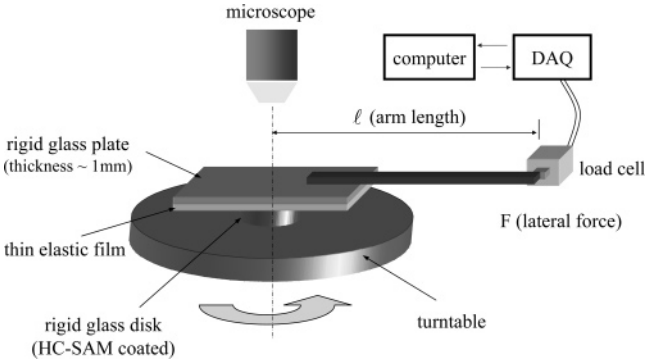

Figure 1. Schematic of the apparatus used for the rotational shear experiment. The load cell (model L2338, Futek Advanced Sensor Technology Inc., Irvine, CA) measures the force (F) resulting from the rotation of the disk (3.8 mm radius and 1 mm thickness) against the PDMS coated glass plate. The rigid glass disk with a low surface energy was prepared by grafting hexadecyl trichlorosilane (HC-SAM; $CH_3(CH_2)_{15}SiCl_3$). The advancing and receding contact angles of water on the HC-SAM coated glass disk were 110° and 104°, respectively. The dimension of the cantilever beam was 60 mm × 5 mm × 1 mm. A computer assisted data acquisition system (model PCI-DAS6035, Measurement Computing Corp., Middleboro, MA) via LabVIEW software allowed the collection of a large amount of data and subsequent processing. The interface between the disk and the film is viewed using an optical microscope (Nikon, model SMZ-2T, Mager Scientific, Dexter, MI) equipped with a charge-coupled device (CCD) video camera (Sony, model XC-75, Optical Apparatus Co., Ardmore, PA).

NY) that was strongly attached to a turntable. The surface of the glass disk is quite smooth, as its root mean square (rms) roughness was found to be ~0.36 nm by atomic force microscopy. The results of friction obtained with such a smooth surface should thus be comparable to those of our previous studies,[4,7] where a silanized smooth silicon wafer of rms roughness 0.2 nm was used. A glass cantilever beam (60 mm × 5 mm × 1 mm) glued to the rigid glass plate rests against a load cell, which measures the force. The only force exerted in the normal direction is by the specimen weight (~10 g), which produces a uniform normal stress of ~2 kPa. The normal stress generated in the rotational shear experiment is in the range of 10−100 kPa, corresponding to the shear stress of 80−800 kPa. We thus ignored the stress due to the weight of the specimen in our analysis of the experimental data.

When a rotational torque is applied to the turntable, the disk rotates along with it, while the film in contact with the disk does not rotate and remains in the suspended state as shown in Figure 1. As one end of the cantilever beam rests against the load cell, it measures the force resulting from the relative displacement of the glass disk and the PDMS film. The resulting angular velocities are measured by timing the revolution of the turntable.

The net external torque is the product of the force (F) measured on the load cell and the arm length (l), which is balanced by the internal torque due to friction acting on each differential area dA on the cross section to maintain a uniform rotational speed.[20] The torque balance yields the following result:

$$Fl = \int_A \sigma(r,\theta) r \, dA \cong \int_0^R 2\pi\sigma(r) r^2 \, dr \qquad (1)$$

where σ is the shear stress and R is the radius of the glass disk. σ in eq 1 is assumed to be solely a function of r. In reality, it may slightly depend on the angle θ of the arm if some asymmetry is present in the system. These details are unimportant in our current studies. The frictional stress for the elastomeric surface, however, depends on the slip velocity. Our previous studies[4,7] show that the shear stress varies with slip velocity following a power law, that is,

$$\sigma = cV^n \qquad (2a)$$

or

$$\sigma = c(2\pi r\omega)^n \qquad (2b)$$

where V is the linear velocity increasing in the radial direction, ω (revolutions/second, rps) is the angular velocity of rotation, and c and n are both constants that need to be found experimentally. Substitution of eq 2 into eq 1 leads to the following expression:

$$Fl = (2\pi)^{n+1}\left(\frac{R^{n+3}}{n+3}\right)c\omega^n \qquad (3)$$

According to eq 3, the torque should increase with the angular rotational speed following a power law. After obtaining both the pre-exponential and the exponential factors from the analysis of the experimental results, the relationship between shear stress and sliding velocity can be obtained from eq 2a.

Results and Discussion

When the rotational torque is applied to the turntable, the friction force increases and the disk begins to rotate on the elastomeric film. During rotation at constant angular velocity (ω), a shear stress is developed at the interface that increases from the center of contact toward the outer edge as the circumferential velocity (V) increases radially ($V = 2\pi r\omega$). When the local shear stress at the interface reaches a critical value, local slip zones may develop at the interface,[22] which are invisible to the naked eye. However, if a normal stress develops due to rotation as well, then an elastic instability at the elastomeric film/disk interface causes the generation of numerous cavitating bubbles that are visible to the eye. We have noticed that normal stress usually develops at the interface due to a slight mismatch of the contact between the PDMS film and the disk. A slight misalignment also promotes the formation of these bubbles. This is particularly the case with thin films. These bubbles rotate along the direction of rotation with a velocity much higher than the rotational speed. We have observed various pattern formations with these bubbles when they are formed. With the increase of the rotational speed, and thus an increase of the shear stress, some of the bubbles that appear near the edge of contact spiral toward the center of contact, whereas some of the bubbles simply rotate concentrically. When numerous bubbles are formed, they may coalesce and establish either a concentric or a spiral-like instability pattern as shown in Figure 2. Through more recent experiments,[23] we have now established that the formation of the spiral instability requires some unique conditions, some of which are discussed in the Appendix.

The reaction force transmitted to the interface creates a tensile force perpendicular to the disk/film interface on one side of the disk but a compressive force on the other. At a critical tensile force, the rigid plate comes off the disk. The stress to failure increases with the shear modulus of the film as $\mu^{1/2}$ but decreases with the thickness as $h^{1/2}$. We will return to this subject later in the paper.

We measured the torque (Fl) with films of various thicknesses and moduli by varying the angular velocity (ω) until the interfacial

(22) Brochard-Wyart, F.; de Gennes, P.-G. *J. Adhes.*, in press.
(23) Choi, S. H.; Chaudhury, M. K. Unpublished results.

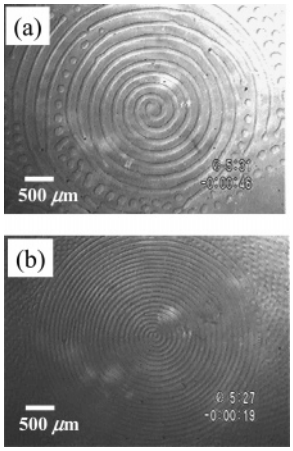

Figure 2. The spiral instability pattern appears at the interface between the rigid glass disk and the thin PDMS film during rotation. The wavelength of instability (i.e., the spacing between the spiral rings) increases with film thickness. (a) $h = 50\ \mu$m, $\mu = 0.9$ MPa and (b) $h = 25\ \mu$m, $\mu = 0.9$ MPa.

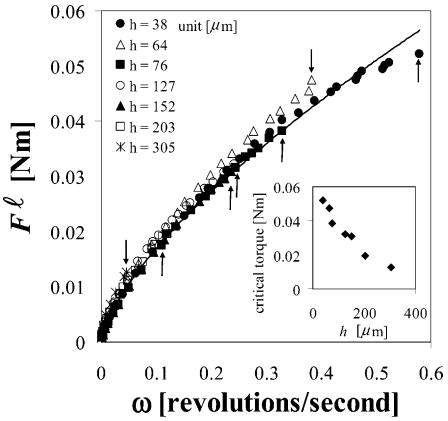

Figure 3. External torque (Fl) as a function of the angular velocity (ω) for different thicknesses of films of shear modulus $\mu = 0.9$ MPa. The experimental parameters are $l = 72$ mm and $R = 3.8$ mm. The external torque increases with the angular velocity following a power law. The solid line represents a fitted curve using the power law regression, and it is given by $Fl = 0.078\omega^{0.65}$. The arrows indicate the critical torque at which the glass disk comes off the thin PDMS film. This critical torque decreases with film thickness as shown in the inset.

fracture occurs. Typical results obtained with a 0.9 MPa film are shown in Figure 3. As expected, the applied torque increases with ω for each film up to a certain angular velocity (or a certain applied torque), beyond which the plate comes out of the disk. As the thickness of the film increases, the critical applied torque for adhesive fracture decreases (inset of Figure 3). The adhesive stability of the interface is thus best for the thinnest films. The applied torque versus angular velocity data for films of various thicknesses nearly superimpose onto a master curve, indicating that the frictional stress itself is independent of film thickness. In other words, the dissipation is restricted to a small region of the interface that is much smaller than any of the thicknesses used in our experiments. It is noteworthy that the elastic instability at the interface seems to have no significant effect on friction either. This result is surprising, as the instability causes a noticeable decrease in the interfacial contact area. However, the instability at the interface, that is, bubble motion, should also increase the energy dissipation by periodic deformation and the relaxation of the bulk of the polymer close to the interface. It is possible that the corresponding increase of friction is somehow compensated by the effect created by the decrease of the contact

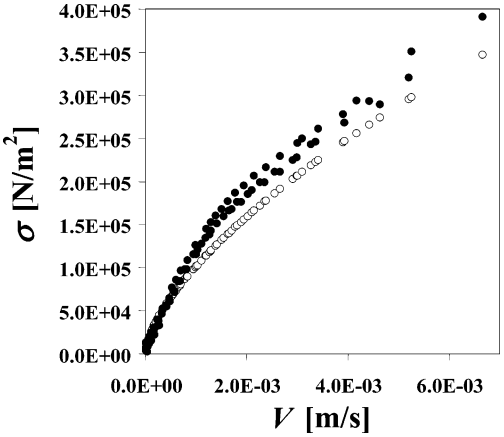

Figure 4. Shear stress versus slip velocity. The open circles are data obtained from the equation $\sigma = 9V^{0.65}$, and the closed circles are the experimental data of Vorvolakos and Chaudhury[4] obtained by sliding a PDMS hemisphere against a silanized silicon wafer.

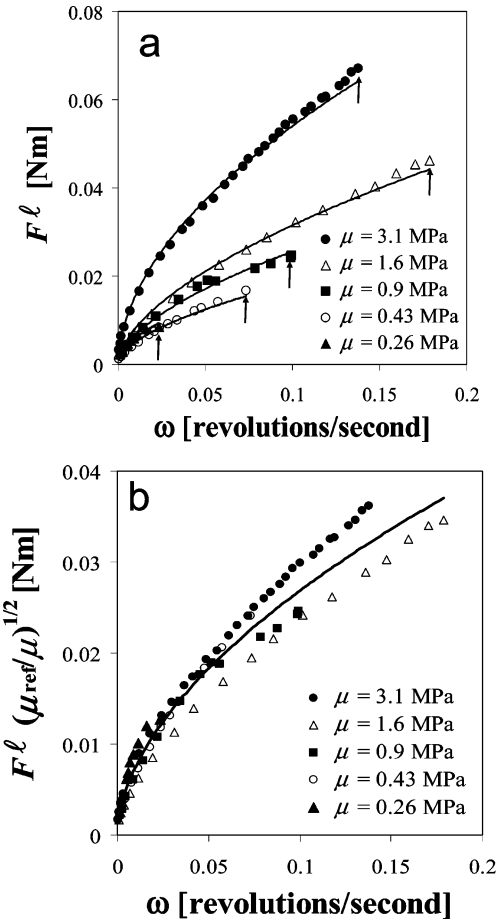

Figure 5. (a) External torque (Fl) as a function of the angular velocity (ω) for various shear moduli of the film (μ), but with the same film thickness ($h = 100\ \mu$m). The experimental parameters are $l = 72$ mm and $R = 3.8$ mm. The external torques increase with the angular velocity following a power law behavior. The arrows indicate the torques at which the glass disk comes off the thin PDMS film. (b) The data shown in Figure 5a are rescaled by multiplying the external torque with the square root of the ratio of an arbitrarily selected reference modulus (0.9 MPa) to the actual modulus.

area. The resultant effect is that the net friction is not dramatically altered from that of a PDMS surface undergoing homogeneous sliding[4] without surface roughening.

From the envelope of all the data summarized in Figure 3, we find that the torque increases with the rotational angular velocity

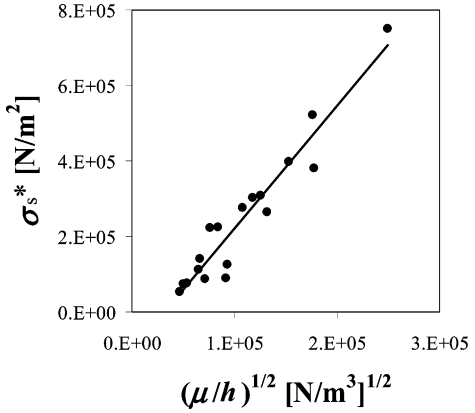

Figure 6. Critical shear stress of an adhesive fracture (σ_s^*) versus $(\mu/h)^{1/2}$. The straight line represents the fitted linear regression ($R^2 = 0.92$), whose slope is 3.3 $(N/m)^{1/2}$.

as $Fl = 0.078\omega^{0.65}$. This, in conjunction with eqs 2 and 3, yields the relationship between the shear stress and the slip velocity as

$$\sigma = 9V^{0.65} \tag{4}$$

where σ is in MPa and V is in m/s. The shear stress obtained from eq 4 is plotted in Figure 4, which is compared with the data obtained by Vorvolakos and Chaudhury[4] by sliding a PDMS hemisphere of the same modulus ($\mu = 0.9$ MPa) on a silanized silicon wafer. The agreement between the shear stress profiles obtained from two sets of measurements, one with a confined geometry and the other with an unconfined geometry, is good.

Figure 5a summarizes the torques related to the rotation of the circular disk against the PDMS films of various shear moduli. As we observed in our previous experiments with an unconfined system,[4,7] the shear stress indeed increases with the modulus of the elastomer. We previously hypothesized that this increase of the shear stress is related to the areal density of segmental contact at the polymer/substrate interface,[7] which varies with the square root of the modulus. Indeed, if we rescale the data by multiplying the external torque with the square root of the ratio of an arbitrarily selected reference modulus ($\mu_{ref} = 0.9$ MPa) to the modulus of the film, all the data nearly collapse onto a single master curve (Figure 5b).

It should also be noted that the critical stress corresponding to adhesive failure decreases with the thickness of the film but increases with the modulus. This result may be understood by carrying out a different kind of torque balance than that shown in eq 1. The reaction force (F) exerted by the load cell on the glass plate and the frictional force acting at the interface in the opposite direction to F create a torque $\sim Fb$ at the interface of contact between the plate and glass disk, with b being the thickness of the plate. The effect of this reaction force can be visualized by the linear translation of the PDMS coated glass plate perpendicular to the lever arm. This torque also creates a tension at one edge of the contact but a compression on the other side. If the tensile stress is σ_n, then the internal torque is on the order of $\sigma_n D^3$ (torque = force × length; force $\sim \sigma_n D^2$, length $\sim D$), with D being the diameter of the disk. Balancing the above two torques yields $Fb \sim \sigma_n D^3$. However, based on eqs 1−3, $Fl \sim \sigma_s D^3$, where σ_s is the shear stress. Thus, we have $\sigma_n \sim (b/l)\sigma_s$. When the normal stress reaches a critical value, that is, $\sigma_n^* \sim (W_a\mu/h)^{1/2}$ (W_a is the work of adhesion),[21,24,25] the disk is expected to come off the thin film. Thus, the shear stress at which the disk separates from the plate is given by the following equation:

$$\sigma_s^* \sim \left(\frac{l}{b}\right)\sqrt{\frac{W_a\mu}{h}} \tag{5}$$

If we combine the data of adhesive failure in all the above experiments, we find that the critical shear stress (σ_s^*) corresponding to such a fracture indeed varies linearly with $(\mu/h)^{1/2}$ (Figure 6), which is consistent with eq 5. Assuming the work of adhesion between PDMS and the glass disk is ~0.04 J/m^2 and using the values of $l \sim 72$ mm and $b \sim 1$ mm, we estimate the slope of the line shown in Figure 6 as 14 $(N/m)^{1/2}$. The experimental slope is, however, 3.3 $(N/m)^{1/2}$. This disagreement is, however, expected, as we have neglected all the prefactors in the derivation of eq 5.

Summary

Rotational shear is a useful method to study friction in thin soft polymer films. The main finding of this study is that the friction in a thin confined film is independent of the film thickness (40−300 μm range) and its value is essentially the same as that found previously for a PDMS hemisphere sliding against a silanized silicon wafer. Even though the surface energy of the silanized glass is the same as that of the silanized silicon wafer, the glass (0.36 nm) is marginally rougher than the silicon wafer (0.2 nm). However, the difference in roughness at this level does not have any noticeable effect on friction. All these results indicate that the frictional processes are confined to a region much smaller than the thickness of any of the films used in these studies. Surface roughening due to elastic instability does not seem to alter friction in a dramatic way either. This could be due to the compensating effects of increased bulk dissipation due to surface roughening and the decrease of friction due to a lower contact area. The way the experiments are designed in this work leads to the fracture between the disk and the thin PDMS film when a critical shear stress is reached. This critical shear stress follows the prediction of standard fracture mechanics; that is, it is proportional to the square root of the ratio of the modulus to the thickness of the film.[21,24,25] Although we have not developed the following idea here, the separation of the disk from the glass plate can be prevented by setting b of eq 5 to zero. This can be accomplished by attaching the cantilever beam on the other side of the glass plate. As suggested by one of the reviewers, a fracture can also be prevented by attaching two lever arms on opposite sides of the glass plate. In this case, one of the lever arms can be supported against a rigid support by a spring, whereas the other arm can rest against the load cell as has been done here. Such a symmetrical configuration provided by the two arms would hinder the interfacial fracture between the disk and the film, thus being useful for studying only friction.

Acknowledgment. This work was supported by the Office of Naval Research (ONR). We thank S. H. Choi for helping J.Y.C. in carrying out the experiments presented in the Appendix. We thank Prof. P. G. de Gennes for his insightful comments about this work. The Appendix of this paper was prepared in response to some comments received from him on the subject of spiral instability.

Appendix

The objective of this Appendix is to provide additional information about the process of bubble cavitation and its motion under a rotational shear at the interface between a thin elastic

(24) Chung, J. Y.; Kim, K. H.; Chaudhury, M. K.; Sarkar, J.; Sharma, A. *Eur. Phys. J. E* **2006**, *20*, 47.
(25) Kendall, K. *J. Phys. D: Appl. Phys.* **1971**, *4*, 1186.

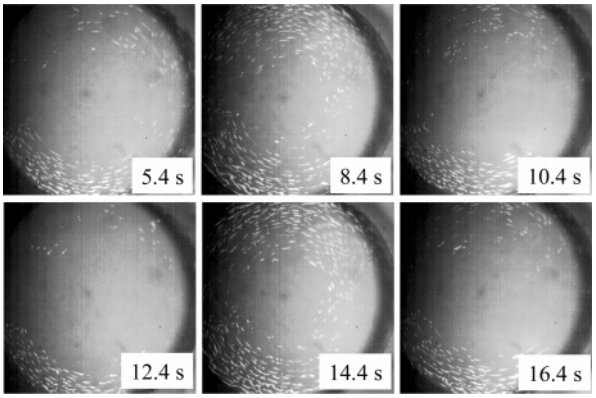

Figure 7. Video microscopic images showing the formation and evolution of bubbles formed at the PDMS/disk interface during rotation. These micrographs were obtained for a film of thickness $h = 38$ μm and shear modulus $\mu = 0.9$ MPa at a rotational angular velocity ~ 0.1 rps.

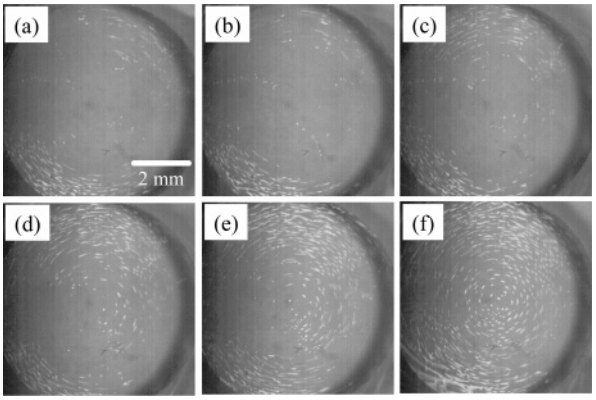

Figure 8. Video microscopic images showing the formation and evolution of bubbles formed at the PDMS/disk interface during rotation at an angular velocity ~ 0.2 rps. Here, film thickness $h = 38$ μm and shear modulus $\mu = 0.9$ MPa. The time interval between images is 0.336 s.

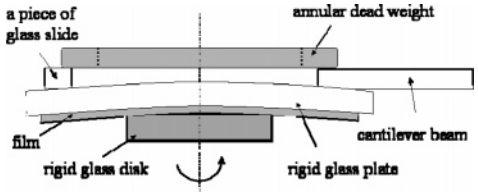

Figure 9. Schematic of the experiment in which a cylindrical weight (90 g) was placed on the rigid glass plate, which causes the plate to bend slightly. All other experimental details are the same as those in Figure 1. Note that the elements illustrated in the figure are not to scale and are highly exaggerated.

film and a rigid glass disk. Figure 7 shows a typical pattern of cavities that are formed during rotation at a relatively moderate speed ($\omega \sim 0.1$ rps). When the elastomeric film is initially placed on top of the rigid glass disk, some bubbles are trapped near the edge of the contact interface. When subjected to steady rotational shear, those bubbles disappear after traveling some distance and new bubbles appear near the edge of contact (see Figure 7). In some cases, a few scattered bubbles are created locally at heterogeneous spots which are caused by impurities or defects at the interface. New bubbles are continuously created from those heterogeneous spots that travel circumferentially.

As the disk continues to rotate, more bubbles are formed at the interface, which again disappear after traveling a certain distance, typically less than a full revolution. It was interesting to find that the formation of these "second generation" bubbles

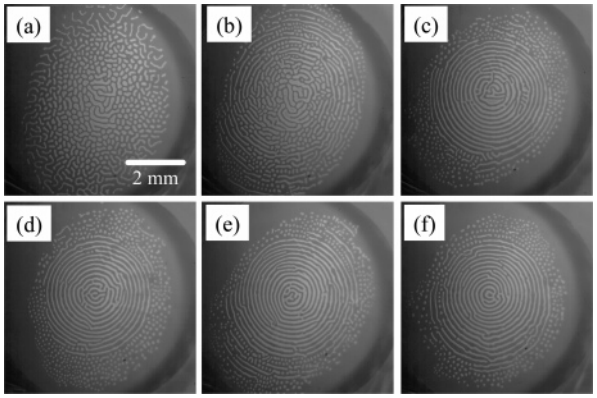

Figure 10. Video microscopic images showing the evolution of patterns at the interface of a PDMS film and a disk under rotational shear. These micrographs were obtained for a film of thickness $h = 51$ μm and shear modulus $\mu = 0.9$ MPa subjected to a normal load of 90 g. Angular velocity ~ 0.07 rps, and time interval between images $= 22$ s.

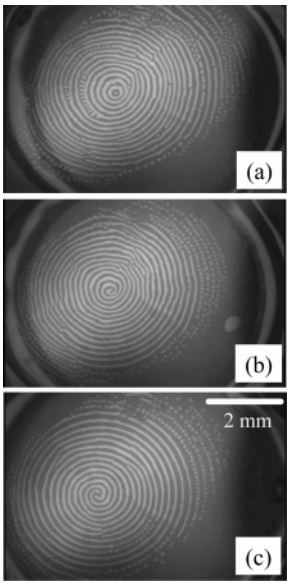

Figure 11. Optical microscopic images showing various patterns at the interface between the film and the disk under rotational shear. All the micrographs were obtained for a film thickness of 51 μm and a shear modulus of 0.9 MPa subjected to a normal load of 90 g. The concentric ring pattern (a) and spiral-like pattern with one origin (b) as well as with two origins (c) can be seen here. Note that the bubble patterns seem to be shifted from the center of rotation, which is due to the fact that the microscope was placed at an angle for better manipulation of the specimens and ease of videography.

is periodic, in that they appear throughout the contact area and then some time later they disappear.

At a relatively higher rotational speed ($\omega \sim 0.2$ rps, see Figure 8), the bubbles appear more densely distributed in significantly larger regions throughout the contact area as compared to those observed under a moderate speed. These bubbles travel azimuthally with a speed much faster than that of the glass disk. Presumably, due to the decaying stress profile field toward the center of contact, the bubbles were forced to travel rapidly along a spiral path toward the center. These bubbles disappear when they become fully developed throughout the entire contact region. This rapid bubble motion results in the stick−slip event that repeats itself periodically as long as the interface stays in contact.

It is evident from the results shown in Figures 7 and 8 that the onset of bubble nucleation strongly depends on the rotational speed and thus on the local circumferential velocity (V), since

$V = 2\pi r\omega$. As pointed out by one of the reviewers, if the onset of instability occurs only when a local velocity is above a certain threshold value (V_c) at a given rotational speed (ω), then we would expect that cavitating bubbles (or stripes) should occur within the annular region $r_c < r < R$, where $r_c = V_c/(2\pi\omega)$. Thus, as the higher rotational speed is applied, the larger annular region is occupied by cavitating bubbles (see Figures 7 and 8).

At a high rotating velocity, the PDMS film slips against the disk in the direction perpendicular to the arm, which is due to a reaction force as discussed in the text. As the rotational speed is increased even further, the bubbles are formed more densely throughout the contact area and eventually they tend to coalesce with each other due to high traffic density. During this period, we often observe a strong tendency of concentric rings or spiral patterns at the interface. We learned that, for the pattern to evolve to a well-developed spiral instability (or concentric ring), certain conditions must be met.

We found that the increase in the normal load also leads to an increased number of bubbles at the interface that promotes different types of pattern formation. This normal force can be internally generated owing to slight mechanical misalignment (translational or rotational) or due to a slight mismatch of the contact between the film and the disk. To test the sensitivity of the normal force, we performed a controlled experiment by placing an annular dead weight on the rigid glass, following the protocol described in ref 17. An annular ring having a weight of 90 g, the inner diameter of which is 4 times larger than the diameter of the glass disk, was placed on top of the rigid glass plate that supported the elastomeric film (see Figure 9). This geometry causes the glass plate to bend slightly and generates a normal force near the center of contact, thus promoting bubble nucleation at the interface.

Upon the rotation of the disk, the randomly distributed bubbles or the wormlike patterns are aligned into well-spaced tracks, as shown in Figure 10. In general, as the rotational speed is increased slowly, bubbles start to elongate azimuthally in the direction of rotation and form locally continuous "bubble tubes". At a higher speed, the bubbles near the center of the rotation are elongated while those on the outward tracks are broken into smaller bubbles. The growing ends of the elongating bubbles are continuously broken into smaller ones at the outward border of the bubble tracks that add new bubbles to these tracks. After some time, the central region is occupied by continuous tracks of elongated bubbles with a characteristic spacing between them.

In some cases, concentric rings are observed toward the center (Figure 11). Although it is still unclear what causes the formation of spiral growth patterns, we believe that some asymmetric load distribution is responsible for it.

LA700501M